Effect of ball milling treatment on the Zn electrode properties in Ni- Zn battery

G. D. Ivanova[1], V. P. Petrova[2], O. K. Petkov[2], B. A. Minchev[2], P. A. Lilov[2], A. K. Stoyanova- Ivanova[2], A. E. Stoyanova[1]

[1]*Institute of Electrochemistry and Energy System "Academician Evgeni Budevski ", Bulgarian Academy of Sciences, Acad. Georgi Bonchev Str, Block 10, 1113 Sofia, Bulgaria*

[2] *Georgi Nadjakov Institute of Solid State Physics, Bulgarian Academy of Sciences, 72 Tzarigradsko Chaussee Blvd., 1784 Sofia, Bulgaria*

This study is focused on the improvement of the properties of the nickel-zinc battery through ball mill treatment of the Zn-electrode active mass. Three zinc electrodes with carbon additive, two of them mixed with conductive ceramic additives from the Bi-Sr-Ca-Cu-O (BSCCO) system with nominal chemical composition $Bi_{1.7}Pb_{0.3}Sr_2CuO_x$ (B(Pb)SCO 2201) and $Bi_{1.7}Pb_{0.3}Sr_2CaCu_2O_x$ (B(Pb)SCCO 2212), were investigated. The phase composition and morphology of the as-prepared samples were characterized by scanning electron microscopy (SEM) and X-ray diffraction (XRD). The conductivity of the Zn electrodes was examined by Potentiostatic Electrochemical Impedance Spectroscopy (PEIS) and it was found that the ball mill treatment of the electrodes with BSCCO additives increases their overall resistance.

Keywords: Ni- Zn battery, through ball mill treatment, Zn-electrode, conductive BSCCO ceramic additives

INTRODUCTION

The nickel-zinc battery is one of the most significant energy storage systems for various electrical applications due to moderate specific energy (55-85 $Whkg^{-1}$), high specific power density (140-200 Wkg^{-1}), high open circuit potential (1.705 V), and nominal cell voltage of 1.6 V [1,2]. These batteries have attractive, such as being low cost, environmentally friendly and having abundant resources of raw materials. However, they have not reached their full potential mostly due to critical problems with the zinc electrode. These problems are attributed to the shape change of the electrode with increasing charge/discharge cycle count, zinc electrode passivation, and dendritic zinc growth leading to short – circuiting of the battery. During the discharge process, zincate ion ($Zn(OH)_4^{2-}$) in the alkaline electrolyte is formed before zinc oxide precipitates. During the charging process, the concentration of zincate ions near the bottom of the electrode decreases and zincate ions are precipitated as zinc oxide when the limit of solubility is reached. This process leads to shape change and formation of zinc dendrites as well as protrusion on the surface of zinc electrode with increasing the number of charge/discharge cycles [3].

Passivation is also another serious problem for deterioration of zinc-based batteries. The passivation of the zinc electrode occurs when the solubility of the zincate ions is exceeded in the electrolyte close to the surface of the zinc electrode, and an insulating ZnO barrier layer is formed on the electrode surface. Due to these issues, short cycle life and/or poor electrochemical performance have limited the wide-range application of Ni-Zn batteries.

There are approaches to solving the existing problem, one of them being the introduction of conductive ceramic additives to the zinc electrode mass. Our previous researches have shown that the nickel-zinc battery cell with zinc electrode whose active mass contain superconducting B(Pb)SCCO (2212) and B(Pb)SCO (2201) ceramic additive exhibits increased cycling and performance stability during prolonged charge-discharge [4-6]. It is supposed that the superconducting powder forms a highly conductive network between the particles of the zinc oxide in the electrode mass, thus improving the electric contact in the power generation material of the zinc electrode. The addition of BSCCO ceramics improves not only the conductivity and electrochemical homogeneity of the electrode mass and reduces the gas evolution (because of the absence of carbon materials with low- overpotential of hydrogen evolution), but it also stabilizes its porous structure [7-9].

The optimization of the zinc electrode mass, including the homogeneous particle distribution of zinc oxide and ceramics, is very important for the robust operation of the battery. The method of electrode preparation can modify the surface morphology and, consequently, the affinity between the particles, which is beneficial to improve the

* To whom all correspondence should be sent.
 E-mail: galia.ivanova@iees.bas.bg

cyclic stability of the electrode. Therefore, the correct choice of active mass preparation has significant effect on the electrochemical properties of the electrode.

A simple effective method to improve the rate capability and reduce the initial voltage delay without compromising the capacity of the active material is the ball milling treatment [10, 11]. Although it may not be as effective as some soft chemical methods that can elaborately tailor the physicochemical nature of the final products, the mechanochemical method is, due to its simplicity and easy operation, attractive and in principle applicable to different electrode materials with poor structural integrity. It is found that the high-energy ball-milling, brings considerable effects on the structure, morphology, and size distribution of the electrode materials, thereby modifying their electrochemical behavior [12, 13].

Improved electrochemical activity (increased capacity, stable cycling behavior, and good rate capability) of $LiMnPO_4$ ball-milled with 8 wt. % acetylene black has been established and this effect may be attributed to enhanced kinetics and structure integrity, which are related to the decreased particle size, expanded unit cell volume, and crystal defects. It is believed that the activity of $LiMnPO_4$ can be further improved given that the ball-milling parameters like time, material/ball ratio, and conductive additive are optimized [2].

Our previous work has shown that the active mass with carbon and B(Pb)SCO 2201 additive has superior particle distribution compared to the other two samples (with B(Pb)SCCO 2212 and without ceramic additive) after ultrasound treatment while the composition of the active mass is preserved [14].

These results and the results, obtained from other authors in different systems [2, 10-13] provoked our interest to conduct similar studies by processing the active mass in a ball mill. The aim of this work is to determine the effect of ball mill treatment on the physicochemical and electrochemical properties of the negative active mass in Ni/Zn cell, as compared with an untreated electrode mass.

EXPERIMENTAL
Preparation of the B(Pb)SCCO conductive ceramic additives

The powder sample of conductive ceramic additives from the Bi-Sr-Ca-Cu-O (BSCCO) system with nominal chemical composition $Bi_{1.7}Pb_{0.3}Sr_2CuO_x$ (B(Pb)SCO 2201) and $Bi_{1.7}Pb_{0.3}Sr_2CaCu_2O_x$ (B(Pb)SCCO 2212) are prepared by the standard solid state reaction. High-

purity (99, 99 %) oxides and carbonates (Bi_2O_3, PbO, CuO, $SrCO_3$ and $CaCO_3$) were used for the production of the Bi-Sr-Ca-Cu-O system samples. The powder is thoroughly mixed, ground and initially heat treated at 780 ºC for 24 hours in air. Afterwards the obtained mass is ground and pressed (5-6 MPa) into round tablets 9.8 mm in diameter and 1.8 mm in thickness. The tablets are then sintered again: B(Pb)SCCO 2212 at 830 ºC for 48 hours and B(Pb)SCO 2201 at 830 ºC for 24 hours in air atmosphere (in accordance with established procedure [15]). BSCCO tablets were ground again and the powder was used as an additive to the active mass.

Preparation of the active mass

An electrode mass was composed of powder ZnO (NZnO50, Anhui Elite Industrial Co., LTD, Hong Kong Elite Industrial Group Limited) (67 %)), acetylene black (14 %) and binding agents – polytetrafluorethylene (PTFE, 5 %) and carboxymethylcellulose (CMC, 14 %). Two other were prepared with acetylene black (7 %), additives – conducting ceramic powder B(Pb)SCO 2201 and B(Pb)SCCO 2212 (7 %) respectively and the same binding agents. The prepared composite of zinc oxide and additives was sequentially plasticized with PTFE suspension and with CMC and mixed manually to form a mushy paste [16]. For better mixing, the active mass was also homogenized in a ball mill for 1 hour at room temperature (23 °C).

Preparation of the zinc electrodes

The pasted zinc electrodes prepared by inserting the zinc paste in the matrix of copper foam (successively covered with tin and zinc) with dimensions 2,0 x 2,0 cm (thickness 0,15 cm) are used for current collector and carrier of the zinc mass. The pasted electrode is dried at 70 ºC for 2 hours and then pressed under 30 MPa for 2 min. The paste was applied to form uniform layer.

Physicochemical characterization of electrode materials

The following methods are used for physicochemical and electrochemical characterization of the investigated substances: X-ray diffraction (XRD), Scanning Electron Microscopy (SEM) and Potentiostatic Electrochemical Impedance Spectroscopy (PEIS).

The samples were examined using a Philips X-ray diffractometer PW 1030 having a θ-2θ Bragg-Brentano geometry, with Cu Kα radiation (30 kV, 20 mA) with a wavelength λ = 1.5406 Å and a scintillation detector. The original radiographs were obtained at room temperature and a constant scan rate and a reflection angle of 2θ in the interval 5 ÷ 90° with a step of 0.04°. The

diffraction patterns obtained were interpreted by the PCPDFWIN database, ICDD, 2002

The microstructure of the prepared active masses was studied by JOEL-200 CX scanning electron microscope (SEM) with LaB$_6$ cathode on the polished cross-section of the samples, at 80 keV.

*Electrochemical impedance spectroscopy measurements*

The electrochemical system SP-200: potentiostat/galvanostat was used to perform potentiostatic electrochemical impedance spectroscopy (PEIS) measurements. The obtained impedance spectra were fitted to an equivalent circuit model using the EC-Lab software. PEIS measurements were taken using the ZnO electrodes as the working electrode (WE) in a three electrode electrochemical cell. The counter-electrode (CE) was a platinum plate. Potential was measured relative to a saturated calomel reference electrode (RE). The applied sine-wave potential amplitude is 10 mV. In some cases a higher potential of 20 or 30 mV was required in order to obtain noise free data. In all experiments the frequency was swept form 1 MHz down to 0.1 Hz. The supporting electrolyte was 7M KOH. Impedance spectra were taken at 25 ºC in order to examine electrode kinetics near working condition.

RESULTS AND DISCUSSION

The XRD patterns of the ball mill and mechanically mixed electrode masses are compared in Fig.1.

Based on XRD analysis of the two electrode masses, containing B(Pb)SCCO additives a single well-crystallized phase of the ceramic is observed. Secondary phases are not detected. The ball mill treatment only affects the active mass with B(Pb)SCO 2201 ceramic. There is a slight broadening of the diffraction peaks, indicating a decrease of the particle size during ball mill processing. In the other two samples, the treatment method has no impact on the structure of the active mass.

The morphology of the active electrode mass is the next parameter that influences the electrode performance. In Figure 2 the SEM images of the Zn active mass with carbon, B(Pb)SCO 2201 and carbon and B(Pb)SCCO 2212 and carbon – additives, treated mechanically and by ball milling are compared.
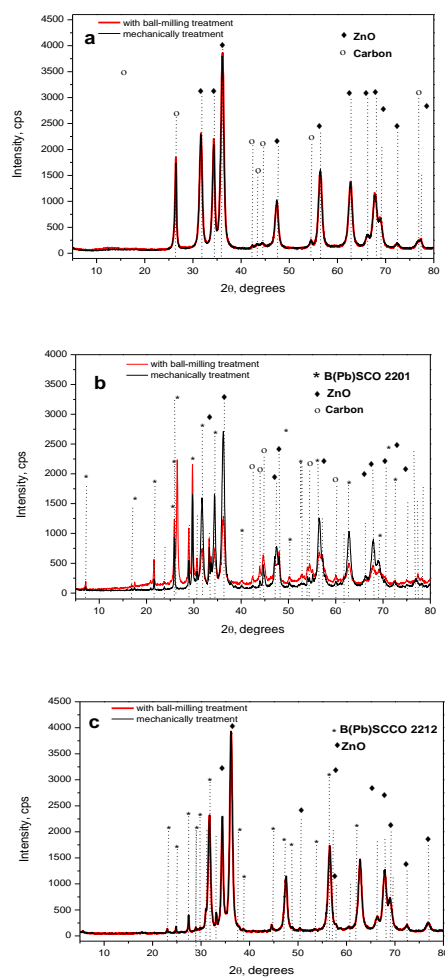
Fig. 1. Powder X-ray diffraction patterns of the Zn active mass with B(Pb)SCO 2201+ carbon (a), B(Pb)SCCO 2212 + carbon (b) and carbon (c), prepared with mechanical (black lines) and ball mill (red lines) mixing

The ball mill assisted mixing of the active mass leads to very good ceramic and carbon particle distribution (Fig. 2). The SEM images of the active mass display a formation of relatively homogenous surface with fine-grained structure. The sample with B(Pb)SCO 2201 shows a particle reduction after ball milling that is consistent with XRD images (Fig. 1b). The results presented so far correlate well with those of our previous studies according to which ultrasound treatment mainly affects the active mass with carbon and B(Pb)SCO 2201 additive [14]. The morphology of the active electrode mass is the next parameter that influences the electrode performance. In Figure 2 the SEM images of the Zn active mass with carbon, B(Pb)SCO 2201 and carbon and B(Pb)SCCO 2212 and carbon – additives, treated mechanically and by ball milling are compared.
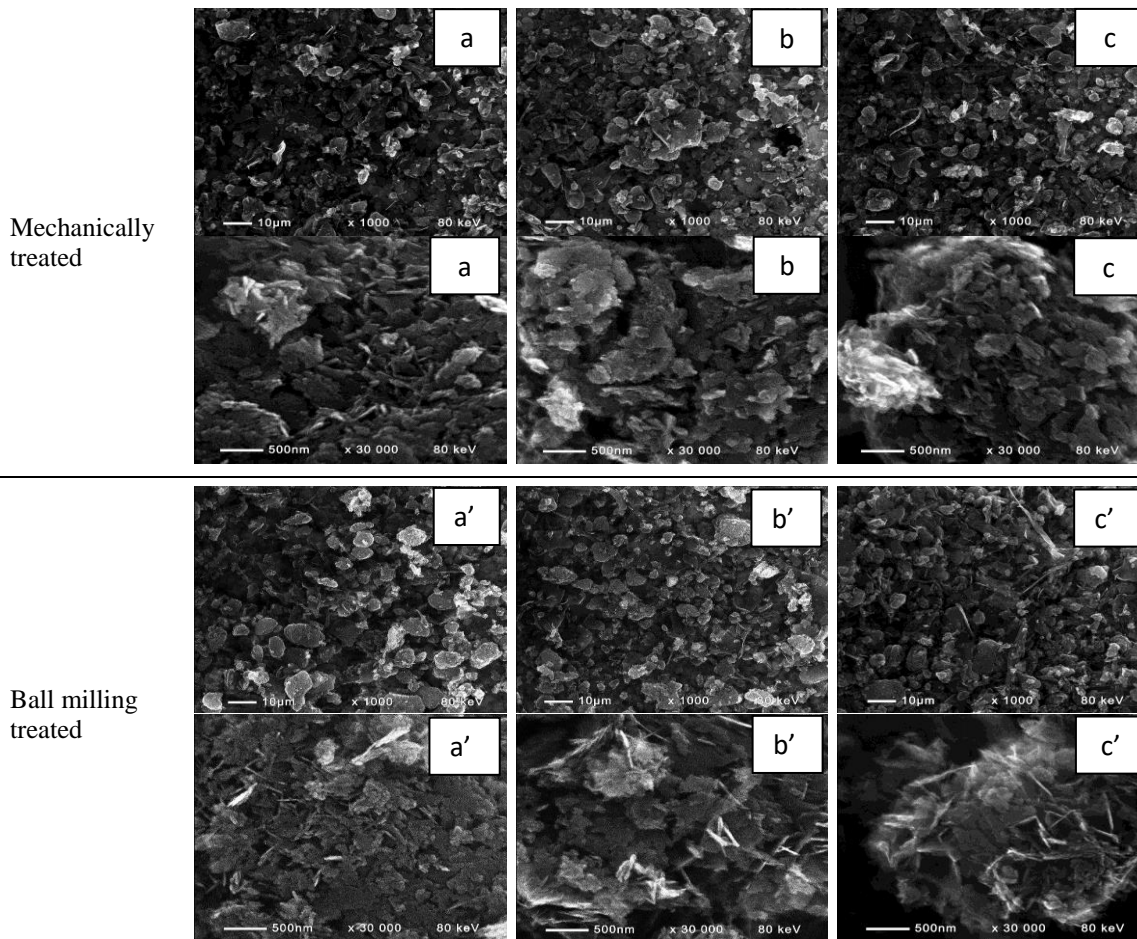
Fig. 2 SEM images of the Zn active mass with carbon (a, a'), B(Pb)SCO 2201+carbon (b, b') and B(Pb)SCCO 2212+carbon (c, c') with mechanical and ball mill treatment

The ball mill assisted mixing of the active mass leads to very good ceramic and carbon particle distribution (Fig. 2). The SEM images of the active mass display a formation of relatively homogenous surface with fine-grained structure. The sample with B(Pb)SCO 2201 shows a particle reduction after ball milling that is consistent with XRD images (Fig. 1b). The results presented so far correlate well with those of our previous studies according to which ultrasound treatment mainly affects the active mass with carbon and B(Pb)SCO 2201 additive [14].

Probably the different structure and composition of the two ceramics is responsible for the observed effect. Electrochemical tests were conducted to interpret these results further. The Nyquist plots of zinc electrodes with carbon and carbon and ceramic additives, mixed in ball mill have been recorded (Fig. 3). These measurements are compatible with our previous studies on the impedance of Zn electrode mass after mechanically and ultrasound treatment [14]. On the graph the electrode resistance is determined by the high frequency intercept of the curves with the real axis. Calculated impedance parameters, using the equivalent circuit

model describing PEIS (Fig. 3, insert) are given in Table 1.
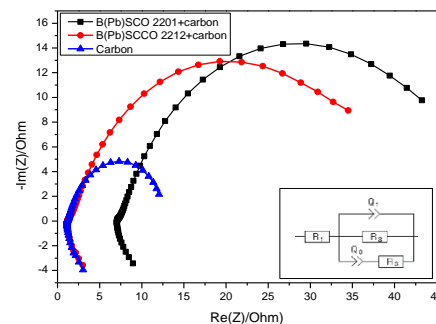
Fig. 3 Nyquist impedance plot of ZnO electrodes with carbon, B(Pb)SCO 2201+carbon and B(Pb)SCCO 2212+carbon at 25°C with ball milling treatment (insert figure - equivalent circuit model for electrode)

The results show that the electrode with B(Pb)SCO 2201 additive exhibits significantly higher resistance, compared to the other two samples. This can be due to the changes in an electronic conduction path in the electrode matrix when treated with a ball mill and respectively to the worsening of its electrochemical characteristics. Not well-chosen ball milling parameters like time,

fluid, material/ball ratio and conductive additive is another possible cause of the obtained effect [17].

Table 1. Calculated impedance parameters of ball mill treated electrodes (the data presented are from measurements taken with an applied potential of 20 mV)

Para-meter	Carbon (C)	B(Pb)SCO 2201+C	B(Pb)SCCO 2212+C
R_1, Ω	1.18	7.05	1.15
Q_1, Fs^{-1}	16.5×10^{-3}	9.08×10^{-3}	9.2×10^{-3}
a_1	0.952	0.708	0.681
R_2, Ω	11.95	43.54	39.41
Q_3, Fs^{-1}	27.5×10^{-3}	1.78×10^{-3}	2.25×10^{-3}
a_3	0.825	0.905	0.938
R_3, Ω	0.65	4.5	3.75

CONCLUSIONS

In this work the effect of the ball mill mixing of the active mass on the Zn- electrode characteristics is discussed. XRD analysis shows that the composition of the active mass is preserved during the grinding process. There is no significant change in the active mass morphology after ball mill treatment. BSCCO additives increase the overall resistance of the electrode, which adversely affects the electrochemical characteristics of the electrode, respectively of the battery. The use of ball mill assisted mixing for preparation of the Zn-electrode active mass is not appropriate in the current conditions until further optimization is done.

REFERENCES

1. G. Payer, O. Ebil, *J. Nanomater.,* **17**, 75-84 (2016).
2. J. Ni, Y. Kawabe, M. Morishita, M. Watada, T. Sakai, *J. Power Sources,* **196**, 8104 – 8109 (2011).
3. G. Cihanoglu, O. Ebil, *J. Turkish Chemical Soc. Chem.*, **5**, 65-84 (2018).
4. G. Ivanova, L. Stoyanov, S. Terzieva, A. Stoyanova-Ivanova, M. Mladenov, D. Kovacheva, R. Raicheff, *BPS*, **14**, 33-34 (2014).
5. G. Ivanova, L. Stoyanov, A. Stoyanova, M. Mladenov, R. Raicheff, *BPS*, **16**, 27-29 (2016).
6. G. Ivanova, A. Stoyanova-Ivanova, D. Kovacheva, A. Stoyanova, *Bulg. Chem. Com.,* **51**, 66 – 72 (2019).
7. G. Ivanova, L. Stoyanov, S. Terzieva, A. Stoyanova-Ivanova, M. Mladenov, D. Kovacheva, R. Raicheff, *Nanosci. Nanotechnol.,,* **14**, 33 (2014).
8. L. Stoyanov, S. Terzieva, A. Stoyanova, A. Stoyanova- Ivanova, M. Mladenov, D. Kovacheva, R. Raicheff, *JPRC,* **2**, 83 - 91 (2016).
9. G. Ivanova, L. Stoyanov, A. Stoyanova, M. Mladenov, R. Raicheff, *Nanosci. Nanotechnol.,* **16**, 27 – 30 (2016).
10. Jun-Ying Huang, Wei-Ren Liu*, J. Taiwan Inst. Chem. E.,* **96**, 205-213(2019).
11. P. Zhouad, J. Weng et. all, *J. Power Sources*, **414**, 210-217 (2019).
12. L. Ning, Y. Wu, S. Fang, E. Rahm, R. Holze, *J. Power Sources*, **133,** 229-242 (2004)
13. M. Gutierrez, F. Garcia-Alvarado, E. Gonzalo, M. Dompablo, *J. Power Sources*, **160**, 523 – 528 (2006).
14. V. Petrova, A. Stoyanova-Ivanova, P. Lilov, O. Petkov, G. Ivanova, B. Karamanova, A. Stoyanova, V. Mikli, *ECS Trans.*, **95**, 227-234 (2019).
15. H. Maeda, Y. Tanaka, M. Fukutomi, T. Asano, *J. Appl. Phys.*, **27,** L209 - L210 (1988).
16. M. Mladenov, R. Raicheff, L. Stoyanov, A. Stoyanova-Ivanova, S. Terzieva, D. Kovacheva, *BG Patent Reg. # 111 646 (*in Bulgarian) (2013).
17. F. Kukurugya, E. Kim, P. Nielsen, L. Horckmans, J. Spooren, K. Broos, M. Quaghebeur, *Hydrometallurgy,* **171**, 245-253 (2017).